OPTICS

Optical selection and sorting of nanoparticles according to quantum mechanical properties

Hideki Fujiwara[1,2], Kyosuke Yamauchi[1], Takudo Wada[3], Hajime Ishihara[3,4]*, Keiji Sasaki[1]*

Optical trapping and manipulation have been widely applied to biological systems, and their cutting-edge techniques are creating current trends in nanomaterial sciences. The resonant absorption of materials induces not only the energy transfer from photons to quantum mechanical motion of electrons but also the momentum transfer between them, resulting in dissipative optical forces that drive the macroscopic mechanical motion of the particles. However, optical manipulation, according to the quantum mechanical properties of individual nanoparticles, is still challenging. Here, we demonstrate selective transportation of nanodiamonds with and without nitrogen-vacancy centers by balancing resonant absorption and scattering forces induced by two different-colored lasers counterpropagating along a nanofiber. Furthermore, we propose a methodology for precisely determining the absorption cross sections for single nanoparticles by monitoring the optically driven motion, which is called as "optical force spectroscopy." This method provides a novel direction in optical manipulation technology toward development of functional nanomaterials and quantum devices.

INTRODUCTION

Nanoparticles and nanomaterials—such as quantum dots, nanocrystals, carbon nanomaterials, molecular aggregates, and metal nanoparticles—have attracted great attention owing to their unique mechanical and quantum mechanical properties and have been used in various photonic, electronic, mechanical, and biomedical devices, such as light emitters, solar cells, photocatalysts, molecular electronics, structural materials, drug delivery, and bioimaging (*1*–*6*). Because these properties of nanoparticles/nanomaterials are strongly influenced by the surrounding environment and are significantly different from the bulk properties, such as quantum size effect, the characterization of individual nanoparticles provides important knowledge for advancing nanomaterial and quantum material sciences. Furthermore, the selection and sorting of single nanoparticles according to their characteristics are essential and desired for the precise design of functional nanostructures and development of single-quantum sensors, single-photon sources, and quantum information devices (*7*, *8*).

Optical trapping and manipulation based on optical forces are promising tools for positioning, transporting, and aligning fine particles without mechanical contacts (*9*, *10*). Optical tweezers proposed by Ashkin *et al.* have been used in various research fields, such as biophysics, cell biology, microfluidics, total analytical systems, and micromechanics (*11*, *12*). Optical sorting of dielectric objects has been developed using holographic optics, flow cytometry, interference technology, and near field photonics (*13*–*15*). Metal nanoparticles can also be separated by optical forces based on the surface plasmon resonances (*16*). However, these techniques are limited to the particle selection by the size and refractive index. The optical gradient and scattering forces exerted on small particles and their dependences on the diameter, wavelength, and relative refractive index are determined by the Mie theory. Furthermore, the reported methods are applicable only to the sorting of submicrometer or larger-sized dielectric particles. Trapping and manipulation of smaller-sized particles remain challenging because the optical force becomes weaker in proportion to the particle volume.

In this study, we demonstrate the optical selection and sorting of nanoparticles according to their quantum mechanical properties. Semiconductor quantum dots exhibit characteristic optoelectronic properties due to the quantum confinement of the electron-hole pairs in the nanovolume (*1*, *2*). Diamond nanoparticles exhibit quantum resonances of point defects (*17*, *18*). The optical forces reflect these quantum mechanical properties of nanoparticles and their optical characteristics (*19*, *20*). The interaction between light and nanomaterials induces not only an energy transfer from the photons to the quantum mechanical motion of the electrons but also a momentum transfer between them. The change in the photon momentum give rise to optical forces, which drive the macroscopic mechanical motion of the nanoparticles. We note that there are three types of optical forces: (i) gradient force arising from the inhomogeneous intensity distribution of the electric field, (ii) dissipative scattering force caused by the real part of the refractive index, and (iii) quantum resonant absorption force exerted on nanomaterials. Therefore, we can realize the characterization and selective manipulation of single nanoparticles having various properties by monitoring and controlling the particle motions. This methodology provides a new direction in optical force technology toward advances in nanomaterial sciences.

RESULTS AND DISCUSSION

Optical trapping and sorting system

To realize the sorting of individual nanoparticles, we use counterpropagating different-colored lasers that can extract the resonant absorption force by cancelling out the scattering forces. The counterpropagating beam systems were constructed using a pair of lenses with large numerical aperture placed opposite to each other (*21*) and the inversely directed evanescent waves (*16*). However, it is difficult

[1]Research Institute for Electronic Science, Hokkaido University, Sapporo, Hokkaido 001-0020, Japan. [2]Department of Electronics and Information Engineering, Hokkai-Gakuen University, Sapporo, Hokkaido 064-0926, Japan. [3]Department of Physics and Electronics, Osaka Prefecture University, Sakai, Osaka 599-8531, Japan. [4]Department of Materials Engineering Science, Osaka University, Toyonaka, Osaka 560-8531, Japan.
*Corresponding author. Email: sasaki@es.hokudai.ac.jp (K.S.); ishi@mp.es.osaka-u.ac.jp (H.I.)

to exclude the influence of the gradient force that easily negates the small effect of the quantum resonance force. Thus, we focused on tapered optical fibers, i.e., nanofibers (*22*, *23*). We prepared a nanofiber with a diameter of several hundred nanometers and length of several millimeters (*24*), which exhibited the characteristics of single-mode propagation, thereby forming an intense evanescent field around the fiber and enabling long-distance propagation while maintaining a tightly focused beam of light. Using these characteristics, a uniform electric field distribution could be generated along the fiber by which the particle motion was restricted to one dimension. In addition, the optical gradient force and thermophoretic force, arising from the temperature gradient (e.g., Soret effect), were exerted in a direction perpendicular to the fiber axis such that the particle motion along the nanofiber was driven only by the resonant absorption and scattering forces. Furthermore, because the momentum of the photons in a waveguide depends on the propagation constants of the individual modes, the single-mode wave in our nanofiber had the constant photon momentum; this provides an ideal platform for analyzing the optical forces exerted on the nanoparticles. On the basis of the balance of the absorption and scattering forces induced by the different-colored lasers counterpropagating along the nanofiber, we succeeded in achieving the selective transportation of single nanoparticles according to the quantum resonant absorption (Fig. 1A).

In addition to the selection and sorting, the proposed system can precisely determine the resonant absorption cross sections of single nanoparticles. Fluorescence and photothermal spectroscopies have been widely used for characterizing single nanoparticles and nanomaterials because of their high sensitivity at the level of single-molecule detection (*25*, *26*). However, these methods probe the relaxation processes emitting a photon and thermal energy, which are regarded as indirect absorption measurements. When the excited states of the materials irreversibly transit to other states without undergoing relaxation processes, such as photochemical reactions, these techniques can no longer observe the resonant absorption. Absorption spectroscopy, which directly measures the excitation processes, is an indispensable tool for analyzing the interaction strengths between light and matter. In particular, the absolute values of the absorption cross sections of single nanoparticles/nanomaterials are essential for experimental physics in material science and are crucial for designing nanostructured materials at a single-quantum state level (*27*). However, it is still challenging to detect extremely small absorption signals of single nanoparticles and nanomaterials. In our method, accurate measurement of quantum resonant absorption is realized by precisely observing the optical force–driven motions of the nanoparticles, called as optical force spectroscopy. This spectroscopy based on the optical momentum change instead of the energy change is conceptually different from the conventional techniques.

Figure 1B illustrates the experimental setup. A nanofiber with a diameter of 400 nm was fabricated from a commercial single-mode optical fiber (*24*). The diameter is constant in the waist part of the fiber over a length of several hundred micrometers. The nanofiber was soaked in an aqueous solution of diamond nanoparticles, i.e., nanodiamonds (NDs). Because nitrogen-vacancy centers (NVCs) in NDs have superior properties, such as no photobleaching, high sensitivity to the surrounding environment, and sharp zero phonon line absorption, they have been gaining attention as luminescent and magnetic-responsive nanomaterials that can be used for biological imaging, sensing, and single-photon source (*17*, *18*). Thus, selection

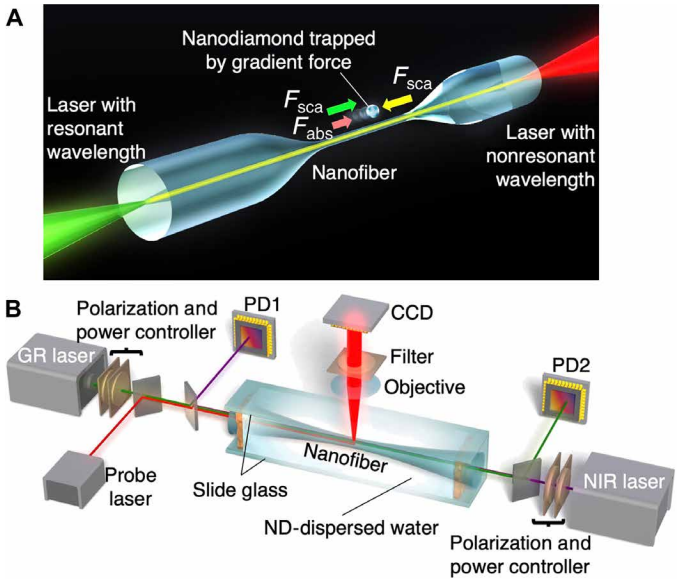

Fig. 1. Absorption detection of single nanoparticles using optical forces. (**A**) Concept of optical force absorption spectroscopy. By monitoring the mechanical motion of a single nanoparticle driven by optical forces, the resonant absorption properties can be analyzed with high sensitivity. Using two different-colored lasers counterpropagating along a nanofiber, a nanoparticle is trapped by the gradient force and transported by the absorption and scattering forces. The laser powers are adjusted to cancel out the scattering forces such that the particle moves depending on the absorption cross section. (**B**) Experimental setup. GR and NIR diode lasers are introduced from both ends of a nanofiber. The laser powers are measured by photodiodes (PD1 and PD2) and controlled by rotational neutral density filters to balance the forces. To record the motion of nanoparticles, a weak red laser is used, and its scattered light is monitored using a microscope-attached charge-coupled device (CCD) camera with filters to cut the strong scattered light of the GR and NIR lasers.

and sorting of NDs with and without NVCs are highly desirable. We prepared two types of NDs; one contained NVCs (>300 per particle), i.e., quantum resonant ND (r-ND), and the other was almost free from the NVCs, i.e., nonresonant ND (n-ND). The diameters of both r-NDs and n-NDs were 50 ± 15 nm. Continuous-wave green (GR; 532 nm) and near-infrared (NIR; 1064 nm) diode lasers were launched from both ends of the nanofiber. The NVCs exhibit absorption at the GR region but not at the NIR region (*28*, *29*). Furthermore, we introduce a weak red laser in the fiber as a probe light (690 nm, 0.1 mW) to monitor the motion of the NDs, which was recorded by an optical microscope equipped with a charge-coupled device (CCD) camera.

Selective transportation of single nanoparticles

Figure 2A depicts the trapping and transportation of a single r-ND, where only the GR laser (70 mW) is incident from the left end of the fiber and the motion of the r-ND is observed in the waist part of the fiber. The result shows that the r-ND is attracted by the gradient force of the evanescent field and moves along the fiber because of the dissipative forces. The particle speed is constant at 110 μm/s (see a trajectory in fig. S1). We evaluate the force exerted on the r-ND as 89 fN by considering the balance between the optical force and viscous drag using the Faxen formula for correcting the effect of the fiber surface [(*23*) and see the Supplementary Materials). When the NIR laser is simultaneously incident from the other end of the fiber

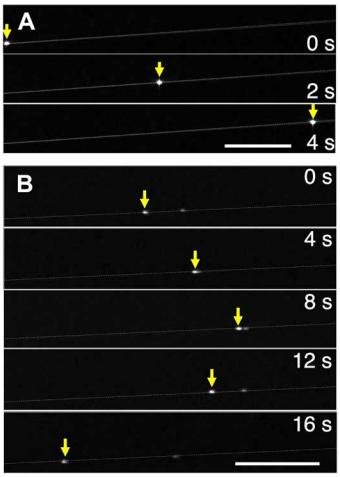

Fig. 2. Transportation and manipulation of a single r-ND along a nanofiber using the GR laser. (**A**) Time-sequential images of the r-ND observed at 2-s intervals. The GR laser is incident from the left end (70 mW). A single r-ND is trapped and transported along the nanofiber at the velocity of 110 μm/s. (**B**) Time-sequential images of the r-ND observed at 4-s interval. The GR laser is incident from the left end of a nanofiber and the NIR laser from the opposite end. The power of the NIR laser is fixed at 250 mW, and the GR laser power is changed from 70 to 0 mW. At approximately 8 s, the optical forces exerted by the two lasers balance each other. The white bar indicates a scale of 100 μm. The dotted line represents the nanofiber position.

(from the right), where the NIR laser power is fixed at 250 mW, and the GR laser power is varied from 70 to 0 mW, we achieve the motion control of a single r-ND (Fig. 2B). At the GR laser power of 70 mW, the r-ND moves toward the propagation direction of the GR laser (from left to right). As the GR laser power decreases, the motion decelerates and subsequently stops (~8 s). On further decreasing the GR laser power, the r-ND moves toward the opposite direction. The motion control experiment for an n-ND is illustrated in the Supplementary Materials (fig. S3).

The dissipative optical force exerted on an r-ND along a nanofiber is composed of two components, namely, absorption and scattering forces (F_{abs}, F_{sca}), which are represented by the absorption and scattering cross sections (σ_{abs}, σ_{sca}), as follows

$$F = F_{abs} + F_{sca} = \frac{n_{eff} I}{c}(\sigma_{abs} + \sigma_{sca}) \quad (1)$$

where I and c represent the intensity and velocity of light in a vacuum, respectively, and n_{eff} is the effective refractive index of the nanofiber (n_{eff} = 1.354 at 532 nm). The scattering cross section for Rayleigh particles is theoretically given by

$$\sigma_{sca} = \frac{128\pi^5 n_2 V^2}{3\lambda^4}\left(\frac{{n_1}^2 - {n_2}^2}{{n_1}^2 - 2{n_2}^2}\right)^2 \quad (2)$$

where n_1 and n_2 are the refractive indices of diamond and surrounding water, respectively, λ is the incident laser wavelength in vacuum, and V is the volume of the particle. In the case of r-NDs including NVCs, σ_{abs} is given by the transition dipole strength of an NVC and the number of NVCs in r-ND. The NIR laser induces only the scattering force, as NVCs exhibit no absorption at 1064 nm.

We perform a motion control experiment for an n-ND without NVCs to measure the balanced powers of the GR and NIR lasers for restricting the motion of the particle. The NIR laser power was fixed at 160 mW, corresponding to the intensity of 108 MW/cm^2 estimated from the mode profile of the nanofiber, while the observed balanced power of the GR laser was 7.61 mW (intensity, 6.06 MW/cm^2). As F_{abs} is not exerted on the n-ND, scattering forces (F_{sca}) by the GR and NIR lasers balance each other. Moreover, σ_{sca} strongly depends on the wavelength (Eq. 2), which is compensated by the large difference between the intensities of the GR and NIR lasers. As σ_{sca} is proportional to the square of the particle volume, the scattering force also changes significantly depending on the particle size. Fortunately, the ratio of the scattering forces at 532 and 1064 nm is constant for any particle size. This is because the volume dependence of σ_{sca} is the same ($\propto V^2$) for both wavelengths. Thus, it is noted that the balanced powers of the two counterpropagating lasers remain unchanged for n-NDs of any size.

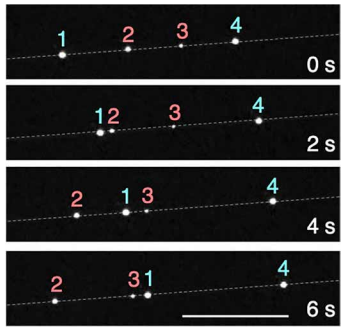

Fig. 3. Selective transportation of r-NDs and n-NDs using counterpropagating GR and NIR lasers. Time-sequential images observed at 2-s intervals. Numbers indicate individual NDs. Particles 1 and 4 represent r-NDs, and particles 2 and 3 represent n-NDs, which is confirmed by the emission of the NVCs. The powers of GR and NIR lasers are set at 7.40 and 160 mW, respectively. The r-NDs move to the right (direction of GR laser propagation), whereas the n-NDs move toward the opposite direction. The white bar indicates a scale of 100 μm. The dashed line represents the nanofiber position.

Furthermore, we demonstrate the selective transportation of r-NDs and n-NDs (Fig. 3 and movie S1). The same experimental setup and nanofiber were used, and the NIR laser power was 160 mW. The GR laser power was adjusted to 7.40 mW to drive different motions of the r-NDs and n-NDs. This value is slightly lower than the balanced power of the n-ND such that the scattering force exerted by the NIR laser is stronger for n-NDs than that by the GR laser, whereas the resonant absorption force on the r-NDs by the GR laser reverses the force strength relation. By switching the probe laser on and off, we can measure the emission from the NVCs and thus distinguish between the r-NDs and n-NDs. The two particles at both ends are r-NDs (numbered 1 and 4) and the other two particles are n-NDs (numbered 2 and 3). Scattered light spots of four NDs have nearly the same intensities when the probe laser is off, while the spots of r-NDs are brighter than the spots of n-NDs in Fig. 3 because the NVC emission is added to the scattered light. The r-NDs slowly move to the right (along the propagation direction of the GR laser), whereas the n-NDs move in the opposite direction (see trajectories in fig. S2). This result clearly demonstrates the selective transportation of NDs according to the quantum resonant absorption of NVCs by using the optical forces.

Determination of the absorption cross section

Next, we analyze the absorption cross section (σ_{abs}) of a single r-ND. We prepared the same experimental conditions and used the same

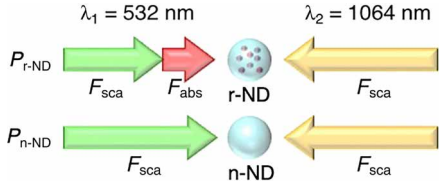

Fig. 4. The balance between dissipative optical forces. The sum of the absorption and scattering forces exerted on the r-ND under GR laser irradiation ($\lambda_1 = 532$ nm) with the power $P_{r\text{-}ND}$ being balanced by the scattering force exerted by the NIR ($\lambda_2 = 1064$ nm) laser. For the n-ND having no absorbers, the scattering forces exerted by the GR laser with $P_{n\text{-}ND}$ and the NIR laser with constant power balance each other. From these balances, the ratio of the absorption and scattering forces on the ND can be determined as $(P_{n\text{-}ND} - P_{r\text{-}ND}):P_{r\text{-}ND}$.

nanofiber that was used for the balanced power measurement of an n-ND. At the NIR laser power of 160 mW, the balanced power of the GR lasers for an r-ND was measured to be 6.75 mW (intensity, 5.37 MW/cm^2). Then, by turning the NIR laser off, the motion of r-NDs driven by the GR laser was observed to determine the strength of the optical force. On the basis of the balance with the viscous drag, the optical force composed of F_{abs} and F_{sca} was calculated as 6.30 fN. As a reference, the data of the n-ND were used for the present absorption analysis. By comparing the balanced powers of the GR laser for the r-ND ($P_{r\text{-}ND}$ = 6.75 mW) and n-ND ($P_{n\text{-}ND}$ = 7.61 mW), we obtain the ratio of F_{abs} and F_{sca} exerted on the r-ND as $(P_{n\text{-}ND} - P_{r\text{-}ND}):P_{r\text{-}ND}$ (Fig. 4) such that the measured optical force on the r-ND (F = 6.30 fN) can be decomposed into F_{abs} = 0.71 fN and F_{sca} = 5.59 fN. This result demonstrates that the absorption and scattering forces exerted on a single r-ND can be separately determined with subfemtonewton order accuracy. Thus, from Eq. 1, we evaluate the σ_{abs} to be 2.9×10^{-14} cm^2. We repeated the measurements for 10 different r-NDs using the same nanofiber to perform the experiments under the same conditions. The average and SD of the evaluated σ_{abs} were 3.3×10^{-14} and 1.1×10^{-14} cm^2, respectively. The deviations in σ_{abs} can be attributed to the variations in the number of NVCs contained in the r-NDs with different sizes and defect densities. The detailed distribution of σ_{abs} and estimated number of NVCs are shown in the Supplementary Materials (see fig. S4).

Here, we emphasize that the present method can detect the absorption cross section in the order of a square nanometer, which is close to those of single molecules (typically as large as 10^{-15} cm^2). Under the diffraction-limited illumination condition, this absorption cross section corresponds to a transmittance of ~10^{-6}. Recently, Kukura *et al.* (*30*) and Celebrano *et al.* (*31*) succeeded in measuring the extremely small absorption using highly sensitive detectors, and the accuracy of their method is comparable with that of our method. However, in their technique, the Rayleigh scattering caused by nanoparticles and nanomaterials attenuates the transmitted light intensity as well such that the absorption signals cannot be extracted separately from the scattering components. In contrast, our proposed optical force spectroscopy can separately determine the absorption and scattering cross sections of single nanoparticles from the momentum change. The sensitivity is not limited by the signal-to-noise ratio of light intensity detection but restricted by the accuracy of the motion detection. Although nanometer-level position sensing techniques are available, the random thermal motion is the main factor that determines the accuracy. If the experiment is performed using superfluid helium at the cryogenic temperature, then the detection accuracy will be ultimately improved.

We demonstrated the selective transportation of single nanoparticles based on the relation between the quantum mechanical properties of nanomaterials and their macroscopic motion driven by the quantum resonant optical forces. This selective transportation is applicable to the precise sorting of nanocrystals, quantum dots, and molecular nanoparticles according to their resonant absorption properties. Optical force spectroscopy directly and sensitively measures the interaction between light and nanoparticles separately from the scattering effects based on the photon momentum change and not the energy change. It is noted that even if the reference nanoparticle having the same parent material but without absorbers is unavailable, the proposed absorption detection can still be achieved (see Materials and Methods). Although we focus on NDs as the samples for the first demonstration, note that other kinds of nanoparticles can be equally interesting targets. Size-selective optical transport of semiconductor quantum dots has been successfully demonstrated (*32*). Furthermore, it was reported that organic dye-doped nanoparticles have unique optical trapping characteristics according to their quantum resonance properties (*33*, *34*). Applying the present technique to these nanomaterials will be our future endeavor. In conclusion, we believe that our scheme can enable a new class of optical force methodologies to investigate the characteristics of advanced nanomaterials and quantum materials and develop state-of-the-art nanodevices.

MATERIALS AND METHODS

Nanodiamonds

We used commercially available NDs having a mean diameter of 50 nm (r-NDs, FND Biotech Inc.; n-NDs, Microdiamant Japan. The absorption of NVCs appears at 532 nm after proton irradiation for fabricating r-NDs; contrarily, n-NDs exhibit no absorption at 532 nm. These were dispersed in pure water with 0.1 weight % surfactant. The concentration was adjusted such that a single ND is trapped by a nanofiber during the experiment.

Fabrication of a nanofiber

A commercially available single-mode optical fiber (780HP, Thorlabs) was used to fabricate a nanofiber. It was heated with a ceramic heater at ~1400°C and stretched at both ends. The waist diameter of the nanofiber used in this study was 400 nm, which remained constant (variation of <2%) over a length of several hundred micrometers. From the mode dispersion curve obtained by the fiber mode analysis, the single-mode propagation is valid when the wavelength of incident light is longer than 360 nm. The fiber was fixed on a glass slide using ultraviolet glue and soaked in a cell filled with an ND-dispersed aqueous solution.

Optical setup

Continuous-wave GR (532 nm) and NIR (1064 nm) diode lasers were introduced from both ends of the fabricated nanofiber. The laser powers were controlled using rotational neutral density filters. To record the motions of the NDs, we introduced a weak red laser (690 nm), and its light, scattered light from the particles, was monitored using a CCD camera. When nanoparticles other than the observed particles are trapped on the fiber, their scattering reduces the laser intensity irradiated on the particle. To avoid this disturbance, the experiments were performed after ensuring no change in the transmitted laser power.

Analysis without the reference particles

When the reference nanoparticle having the same parent material but containing no absorbers is unavailable, the proposed absorption detection can still be realized by the following method: The measurement of the balanced laser powers for the reference particle is replaced by the calculation of the ratio of the scattering cross sections at two different wavelengths (using Eq. 2). When the refractive index of the parent material is constant at two laser wavelengths, the ratio of the scattering cross sections can be obtained using the inverse fourth power law. Using this value, we can determine the balanced laser powers for the virtual nonabsorbing particle. We analyzed the same data for 10 r-NDs as the abovementioned experiments but without using the data for n-NDs; consequently, the absorption cross sections were determined as $(3.8 \pm 1.0) \times 10^{-14}$ cm^2. The variation from the above value [$(3.3 \pm 1.1) \times 10^{-14}$ cm^2] would have been caused by a deviation from the Rayleigh scattering theory (Eq. 2) owing to the shape, size, and refractive index of the particles, as well as the random and systematic errors in the measurements.

SUPPLEMENTARY MATERIALS

Supplementary material for this article is available at http://advances.sciencemag.org/cgi/content/full/7/3/eabd9551/DC1

REFERENCES AND NOTES

1. P. Michler, A. Imamoğlu, M. D. Mason, P. J. Carson, G. F. Strouse, S. K. Buratto, Quantum correlation among photons from a single quantum dot at room temperature. *Nature* **406**, 968–970 (2000).
2. Q. Sun, Y. A. Wang, L. S. Li, D. Wang, T. Zhu, J. Xu, C. Yang, Y. Li, Bright, multicoloured light-emitting diodes based on quantum dots. *Nat. Photonics* **1**, 717–722 (2007).
3. I. Robel, V. Subramanian, M. Kuno, P. V. Kamat, Quantum dot solar cells. Harvesting light energy with CdSe nanocrystals molecularly linked to mesoscopic TiO_2 films. *J. Am. Chem. Soc.* **128**, 2385–2393 (2006).
4. M. B. J. Roeffaers, B. F. Sels, H. Uji-I, F. C. De Schryver, P. A. Jacobs, D. E. De Vos, J. Hofkens, Spatially resolved observation of crystal-face-dependent catalysis by single turnover counting. *Nature* **439**, 572–575 (2006).
5. M. Prato, [60]Fullerene chemistry for materials science applications. *J. Mater. Chem.* **7**, 1097–1109 (1997).
6. X. Shi, K. Ueno, T. Oshikiri, Q. Sun, K. Sasaki, H. Misawa, Enhanced water splitting under modal strong coupling conditions. *Nat. Nanotechnol.* **13**, 953–958 (2018).
7. P. Frantsuzov, M. Kuno, B. Jankó, R. A. Marcus, Universal emission intermittency in quantum dots, nanorods, and nanowires. *Nat. Phys.* **4**, 519–522 (2008).
8. C. L. Degen, F. Reinhard, P. Cappellaro, Quantum sensing. *Rev. Mod. Phys.* **89**, 035002 (2017).
9. A. Ashkin, J. M. Dziedzic, J. E. Bjorkholm, S. Chu, Observation of a single-beam gradient force optical trap for dielectric particles. *Opt. Lett.* **11**, 288–290 (1986).
10. K. Sasaki, M. Koshioka, H. Misawa, N. Kitamura, H. Masuhara, Pattern formation and flow control of fine particles by laser-scanning micromanipulation. *Opt. Lett.* **16**, 1463–1465 (1991).
11. A. Ashkin, J. M. Dziedzic, Optical trapping and manipulation of viruses and bacteria. *Science* **235**, 1517–1520 (1987).
12. A. Ashkin, K. Schütze, J. M. Dziedzic, U. Euteneuer, M. Schliwa, Force generation of organelle transport measured *in vivo* by an infrared laser trap. *Nature* **348**, 346–348 (1990).
13. M. P. MacDonald, G. C. Spalding, K. Dholakia, Microfluidic sorting in an optical lattice. *Nature* **426**, 421–424 (2003).
14. M. Righini, A. S. Zelenina, C. Girard, R. Quidant, Parallel and selective trapping in a patterned plasmonic landscape. *Nat. Phys.* **3**, 477–480 (2007).
15. Y. Shi, S. Xiong, L. K. Chin, J. Zhang, W. Ser, J. Wu, T. Chen, Z. Yang, Y. Hao, B. Liedberg, P. H. Yap, D. P. Tsai, C.-W. Qiu, A. Q. Liu, Nanometer-precision linear sorting with synchronized optofluidic dual barriers. *Sci. Adv.* **4**, eaao0773 (2018).
16. M. Ploschner, T. Čižmár, M. Mazilu, A. Di Falco, K. Dholakia, Bidirectional optical sorting of Gold nanoparticles. *Nano Lett.* **12**, 1923–1927 (2012).
17. A. M. Schrand, S. S. Ciftan Hens, O. A. Shenderova, Nanodiamond particles: Properties and perspectives for bioapplications. *Crit. Rev. Solid State Mater. Sci.* **34**, 18–74 (2009).
18. S. Prawer, A. D. Greentree, Diamond for quantum computing. *Science* **320**, 1601–1602 (2008).
19. T. Iida, H. Ishihara, Theoretical study of the optical manipulation of semiconductor nanoparticles under an excitonic resonance condition. *Phys. Rev. Lett.* **90**, 057403 (2003).
20. H. Ajiki, T. Iida, T. Ishikawa, S. Uryu, H. Ishihara, Size and orientation-selective optical manipulation of single-walled carbon nanotubes: A theoretical study. *Phys. Rev. B* **80**, 115437 (2009).
21. M. G. Donato, O. Brzobohatý, S. H. Simpson, A. Irrera, A. A. Leonardi, M. J. Lo Faro, V. Svak, O. M. Maragò, P. Zemánek, Optical trapping, optical binding, and rotational dynamics of Silicon nanowires in counter-propagating beams. *Nano Lett.* **19**, 342–352 (2019).
22. M. Cai, K. Vahala, Highly efficient optical power transfer to whispering-gallery modes by use of a symmetrical dual-coupling configuration. *Opt. Lett.* **25**, 260–262 (2000).
23. A. Maimaiti, V. G. Truong, M. Sergides, I. Gusachenko, S. N. Chormaic, Higher order microfibre modes for dielectric particle trapping and propulsion. *Sci. Rep.* **5**, 9077 (2015).
24. H. Takashima, K. Kitajima, Y. Tanaka, H. Fujiwara, K. Sasaki, Efficient optical coupling into a single plasmonic nanostructure using a fiber-coupled microspherical cavity. *Phys. Rev. A* **89**, 021801 (2014).
25. S. T. Hess, T. P. K. Girirajan, M. D. Mason, Ultra-high resolution imaging by fluorescence photoactivation localization microscopy. *Biophys. J.* **91**, 4258–4272 (2006).
26. A. Gaiduk, M. Yorulmaz, P. V. Ruijgrok, M. Orrit, Room-temperature detection of a single molecule's absorption by photothermal contrast. *Science* **330**, 353–356 (2010).
27. C. A. Leatherdale, W.-K. Woo, F. V. Mikulec, M. G. Bawendi, On the absorption cross section of CdSe Nanocrystal quantum dots. *J. Phys. Chem. B* **106**, 7619–7622 (2002).
28. T.-L. Wee, Y.-K. Tzeng, C.-C. Han, H.-C. Chang, W. Fann, J.-H. Hsu, K.-M. Chen, Y.-C. Yu, Two-photon excited fluorescence of nitrogen-vacancy centers in proton-irradiated type Ib diamond. *J. Phys. Chem. A* **111**, 9379–9386 (2007).
29. H.-C. Lu, Y.-C. Peng, S.-L. Chou, J.-I. Lo, B.-M. Cheng, H.-C. Chang, Far-UV-excited luminescence of nitrogen-vacancy centers: Evidence for diamonds in space. *Angew. Chem. Int. Ed.* **56**, 14469–14473 (2017).
30. P. Kukura, M. Celebrano, A. Renn, V. Sandoghdar, Single molecule sensitivity in optical absorption at room temperature. *J. Phys. Chem. Lett.* **1**, 3323–3327 (2010).
31. M. Celebrano, P. Kukura, A. Renn, V. Sandoghdar, Single-molecule imaging by optical absorption. *Nat. Photonics* **5**, 95–98 (2011).
32. K. Inaba, K. Imaizumi, K. Katayama, M. Ichimiya, M. Ashida, T. Iida, H. Ishihara, T. Itoh, Optical manipulation of CuCl nanoparticles under an excitonic resonance condition in superfluid helium. *Phys. Stat. Sol. (B)* **243**, 3829–3833 (2006).
33. T. Kudo, H. Ishihara, H. Masuhara, Resonance optical trapping of individual dye-doped polystyrene particles with blue- and red-detuned lasers. *Opt. Express* **25**, 4655–4664 (2017).
34. S. Ito, M. Mitsuishi, K. Setoura, M. Tamura, T. Iida, M. Morimoto, M. Irie, H. Miyasaka, Mesoscopic motion of optically trapped particle synchronized with photochromic reactions of diarylethene derivatives. *J. Phys. Chem. Lett.* **9**, 2659–2664 (2018).

Acknowledgments

Funding: The authors acknowledge the funding received from JSPS KAKENHI (grant numbers JP16H06504, JP16H06506, JP18H03882, JP18H05205, JP17K05016, and JP19H04529) and the Cooperative Research Program of "Network Joint Research Center for Materials and Devices." **Author contributions:** H.I. and K.S. developed the concept and supervised the experiments. K.Y., H.F., and K.S. conducted the experiments. H.I. and T.W. theoretically elucidated the phenomena. H.F., K.Y., T.W., H.I., and K.S. participated in discussion of the results. H.F., H.I., and K.S. prepared the manuscript. **Competing interests:** The authors declare that they have no competing interests. **Data and materials availability:** All data needed to evaluate the conclusions in the paper are present in the paper and/or the Supplementary Materials. Additional data related to this paper may be requested from the authors.

Submitted 22 July 2020
Accepted 23 November 2020
Published 13 January 2021
10.1126/sciadv.abd9551

Citation: H. Fujiwara, K. Yamauchi, T. Wada, H. Ishihara, K. Sasaki, Optical selection and sorting of nanoparticles according to quantum mechanical properties. *Sci. Adv.* **7**, eabd9551 (2021).